

Robust Hovering Control of a Quadrotor Using Acceleration Feedback

Gokhan Alcan^{1,2} and Mustafa Unel^{1,2}

Abstract—This paper presents a novel acceleration feedback control method for robust hovering of a quadrotor subject to aerodynamic disturbances. An acceleration based disturbance observer (ABDOB) is designed to reject disturbances acting on the positional dynamics of the quadrotor. In order to provide high stiffness against disturbances acting on the attitude dynamics, a nested position, velocity and inner acceleration feedback control structure that utilizes PID and PI type controllers is developed. To obtain reliable angular acceleration information, a cascaded estimation technique based on an extended Kalman filter (EKF) and a classical Kalman filter (KF) is proposed. EKF estimates the Euler angles and gyro biases by fusing the data from gyroscope, accelerometer and magnetometer. Compensated gyro data are then fed into a Kalman filter whose process model is derived from Taylor series expansion of angular velocities and accelerations where angular jerks are considered as stochastic inputs. The well-known kinematic relation between Euler angular rates and angular velocities is employed to estimate reliable Euler accelerations. Estimated Euler angles, rates and accelerations are then used as feedback signals in the nested attitude control structure. Performance of the proposed method is assessed by a high fidelity simulation model where uncertainties in the sensor measurements, e.g. sensor bias and noise, are also considered. Developed controllers that utilize estimated acceleration feedback provide extremely robust hovering results when the quadrotor is subject to wind gusts generated by Dryden wind model. Simulation results show that utilization of acceleration feedback in hovering control significantly reduces the deviations in the x-y position of the quadrotor.

I. INTRODUCTION

Vertical Take-Off and Landing (VTOL) vehicles are currently being used in many civilian and military applications due to their great advantages including flight capabilities, low-cost development and easy-to-use structures. To carry out most of these applications, hovering at a given point and maintaining that position by rejecting the external disturbances are very crucial tasks for VTOL type UAVs.

Rejection of external disturbances through velocity based disturbance observers were considered in hover and position control of a tilt-wing UAV by Hancer et al. [1], [2]. Zhang et al. [3] designed an extended observer to estimate time-varying and non-vanished disturbances and used a modified sliding mode term for the attitude control of a quadrotor based on these estimates. Waslander and Wang [4] modeled the wind velocity experienced by the quadrotor as a Dryden model to estimate the disturbance and improve the positioning accuracy. Tayebi and McGilvray [5] developed a new

quaternion-based feedback control scheme for exponential attitude stabilization of a quadrotor that is based on the compensation of the Coriolis and gyroscopic torques, and PD² feedback. Kim et al. [6] obtained a rigorous dynamic model of a quadrotor in the inertial reference and body frames and proposed a robust hovering control method based on disturbance observer and vision based localization.

In addition to disturbance observers (DOB) and linear controllers, several nonlinear control structures were also proposed in the literature. Yildiz et al. [7], [8] developed position control of a quad tilt-wing UAV via a nonlinear hierarchical adaptive control approach which consists of a model reference adaptive controller (MRAC) to produce virtual control inputs for position dynamics and a nonlinear adaptive controller for controlling the attitude/orientation dynamics. Cabecinhas et al. [9] designed a nonlinear adaptive state feedback controller to steer a quadrotor along a predefined path in the presence of constant wind disturbances. Rudin et al. [10] proposed a nonlinear hierarchical controller that can be implemented on a small microcontroller for attitude control of a quadrotor helicopter. Model uncertainties were estimated based on a time-delay control approach and an anti-windup integrator was employed to enhance the robustness of the flight. Pounds et al. [11] proposed a nonlinear attitude stabilizer for low-cost aerial robotic vehicles that includes attitude estimation as well. Carrillo et al. [12] compared three nonlinear controllers including backstepping, nested saturations and sliding modes that employed visual feedback to stabilize the position of a quadrotor and selected controllers were tested in real-time experiments.

Alternatively, vision based solutions have also been exploited to enhance the hovering and positioning performances of UAVs [13]. Bin et al. [14] utilized optical flow in a PD controller to obtain position and velocity feedback for autonomous hovering control of a nano-quadrotor. Lim et al. [15] employed a single-chip strapdown optical flow sensor on a micro quadrotor that can carry only a few dozen grams of payload, and presented an autonomous hovering flight control based on sensor fusion and linear controllers. Azrad et al. [16] presented a vision based control system for Micro Air Vehicles (MAV) that combines Kalman filters to estimate relative pose and a nonlinear controller to track and hover above the target.

Disturbance rejection capability of acceleration control was first discovered by Hori [17], [18] and enhanced by Schmidt and Robert [19]. Han et al. [20] proposed a new predictive estimator for angular acceleration called Newton Predictor Enhanced Kalman Filter (NPEKF) and based on the estimated acceleration, an acceleration feedback control was

¹Faculty of Engineering and Natural Sciences, Sabanci University, Tuzla, Istanbul, Turkey

²Integrated Manufacturing Technologies Research and Application Center, Sabanci University, Tuzla, Istanbul, Turkey
{gokhanalcan, munel}@sabanciuniv.edu

developed for a 2-DOF direct-drive manipulator. Insperger et al. [21] used proportional-derivative-acceleration (PDA) feedback in a model for human postural balance and showed the improvement induced by acceleration feedback. Tomic [22] utilized acceleration based disturbance observation with a boundary-layer integral sliding mode control in attitude control of small UAVs to reject modeling uncertainties and external disturbances. Jeong et al. [23] designed an acceleration-based disturbance observer (ABDOB) for robust attitude control of a quadrotor system where acceleration is obtained by simple differentiation of gyro readings.

Performing surveillance tasks under windy conditions requires robust stabilization of the VTOL vehicles through hover control. In this paper, we develop a robust hovering controller for a quadrotor that utilizes acceleration feedback both in position and attitude control loops. In order to reject disturbances acting on the positional or translational dynamics of the vehicle, an acceleration based disturbance observer (ABDOB) is employed. Furthermore, a nested position, velocity and inner acceleration feedback control is proposed to stabilize the quadrotor against the disturbances acting on the attitude dynamics. Since inner acceleration control requires reliable angular accelerations, an extended Kalman filter (EKF) and a classical Kalman filter (KF) are combined in a cascaded structure to estimate angular accelerations in body frame. In constructing the process model for KF, angular jerks are assumed to be constant stochastic inputs. Reliable Euler accelerations are estimated by using the well-known kinematic relation between Euler rates and angular velocities. Estimated Euler angles, velocities and accelerations are then utilized in attitude stabilization. Dryden wind model is used to generate aerodynamic disturbance forces and moments. The proposed control method is verified by simulations performed on a high fidelity simulator where sensor measurements are corrupted by uncertainties such as bias and noise.

The paper is organized as follows: In Section II, mathematical model of a quadrotor is provided. Estimation of Euler angles, rates and accelerations via sensor fusion is presented in Section III. Section IV describes the hovering control of the quadrotor using acceleration feedback. Simulation results and discussions are presented in Section V. Finally Section VI concludes the paper with some remarks and indicates possible future directions.

II. MODELING OF A QUADROTOR

Conventionally, positional dynamics of UAVs are expressed with respect to a fixed inertial reference frame (world frame) and rotational or attitude dynamics are written with respect to a body fixed frame attached to the UAV (Fig. 1).

Since the quadrotor can be modeled as a rigid body, its dynamics can be written in matrix-vector form as [24], [25]:

$$M\dot{\zeta} + C(\zeta)\zeta = G + O(\zeta)\omega + E(\xi)\omega^2 + D(\zeta, \xi) \quad (1)$$

where ζ is the generalized velocity vector and it is defined as

$$\zeta = [\dot{X}, \dot{Y}, \dot{Z}, p, q, r]^T \quad (2)$$

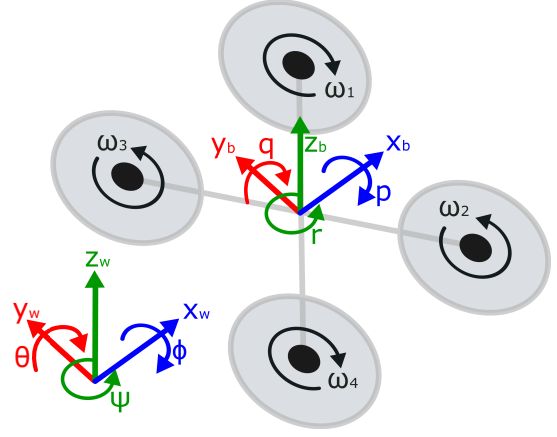


Fig. 1. Quadrotor body frame and the world frame

where $\dot{X}, \dot{Y}, \dot{Z}$ are linear velocities expressed in the world frame, p, q, r are angular velocities expressed in the body frame. Position and orientation of the quadrotor with respect to the world frame is defined as

$$\xi = [X, Y, Z, \phi, \theta, \psi]^T \quad (3)$$

The relation between ζ and ξ is given by the following Jacobian transformation

$$\dot{\xi} = J\zeta \Rightarrow \begin{bmatrix} \dot{X} \\ \dot{Y} \\ \dot{Z} \\ \dot{\phi} \\ \dot{\theta} \\ \dot{\psi} \end{bmatrix} = \begin{bmatrix} [I_{3 \times 3}] & [0_{3 \times 3}] \\ [0_{3 \times 3}] & \begin{bmatrix} 1 & s_\phi t_\theta & c_\phi t_\theta \\ 0 & c_\phi & -s_\phi \\ 0 & s_\phi/c_\theta & c_\phi/c_\theta \end{bmatrix} \end{bmatrix} \begin{bmatrix} \dot{X} \\ \dot{Y} \\ \dot{Z} \\ p \\ q \\ r \end{bmatrix} \quad (4)$$

where $I_{3 \times 3}$ and $0_{3 \times 3}$ are 3×3 identity and zero matrices, respectively. $s_{(\cdot)}$, $c_{(\cdot)}$ and $t_{(\cdot)}$ are abbreviations for trigonometric sine, cosine and tangent functions.

The mass-inertia matrix, M , the Coriolis-centripetal matrix, $C(\zeta, \xi)$, the gravity term, G , the gyroscopic term, $O(\zeta)\omega$ and the system actuator vector, $E(\xi)\omega^2$ are defined as follows:

$$M = \begin{bmatrix} mI_{3 \times 3} & 0_{3 \times 3} \\ 0_{3 \times 3} & \text{diag}(I_{xx}, I_{yy}, I_{zz}) \end{bmatrix} \quad (5)$$

where m is the mass of the vehicle, I_{xx}, I_{yy} and I_{zz} are the moments of inertia around body x, y, z axes, respectively.

$$C(\zeta) = \begin{bmatrix} [0_{3 \times 3}] & [0_{3 \times 3}] \\ [0_{3 \times 3}] & \begin{bmatrix} 0 & I_{zz}r & -I_{yy}q \\ -I_{zz}r & 0 & I_{xx}p \\ I_{yy}q & -I_{xx}p & 0 \end{bmatrix} \end{bmatrix} \quad (6)$$

$$G = [0, 0, -mg, 0, 0, 0]^T \quad (7)$$

$$O(\zeta)\omega = \begin{bmatrix} 0_{3 \times 1} \\ J_{prop} \begin{pmatrix} 0_{3 \times 1} \\ -q \sum_{i=1}^4 \eta_i \omega_i \\ p \sum_{i=1}^4 \eta_i \omega_i \\ 0 \end{pmatrix} \end{bmatrix} = \begin{bmatrix} 0_{3 \times 1} \\ -J_{prop} q \omega_p \\ J_{prop} p \omega_p \\ 0 \end{bmatrix} \quad (8)$$

where J_{prop} is the rotational inertia of the rotors about their rotation axes, $\eta_{(1,2,3,4)} = 1, -1, -1, 1$, ω_i is the rotor rotational speed and $\omega_p = \omega_1 - \omega_2 - \omega_3 + \omega_4$.

$$E(\xi)\omega^2 = \begin{bmatrix} (c_\phi s_\theta c_\psi + s_\phi s_\psi)u_1 \\ (c_\phi s_\theta s_\psi - s_\phi c_\psi)u_1 \\ (c_\phi c_\theta)u_1 \\ u_2 \\ u_3 \\ u_4 \end{bmatrix} \quad (9)$$

where,

$$u_1 = k(\omega_1^2 + \omega_2^2 + \omega_3^2 + \omega_4^2) \quad (10)$$

$$u_2 = kl_s(\omega_1^2 - \omega_2^2 + \omega_3^2 - \omega_4^2) \quad (11)$$

$$u_3 = kl_l(-\omega_1^2 - \omega_2^2 + \omega_3^2 + \omega_4^2) \quad (12)$$

$$u_4 = k\lambda(\omega_1^2 - \omega_2^2 - \omega_3^2 + \omega_4^2) \quad (13)$$

In these equations, k is the lift/thrust coefficient, l_s is the rotor distance to the center of gravity (cog) along the y axis, l_l is the rotor distance to cog along the x axis, and λ is the torque/force ratio.

Motor thrusts are modeled as

$$F_i = k\omega_i^2 \quad (14)$$

$D(\zeta, \xi)$ term in (1) denotes the aerodynamic disturbances acting on the vehicle. In this study, Dryden wind model [4] is employed to model aerodynamic disturbances. This model defines linear and angular velocities of the wind as a sum of sinusoidal excitations by using the altitude and the speed of the UAV, and wind forces and moments are generated by simply scaling these wind velocities with some appropriate weights [1].

III. ESTIMATION OF EULER ANGLES, RATES AND ACCELERATIONS USING SENSOR FUSION

Although acceleration feedback has a tremendous impact on rejecting external disturbances (Hori [17], Schmidt and Robert [19]), obtaining angular acceleration is not a trivial task. We propose a novel cascaded estimation framework (Fig. 2) based on Kalman filters [26] for reliably estimating Euler angles, rates and accelerations.

Proposed method includes an extended Kalman filter as the initial step to estimate quadrotor attitude angles (ϕ, θ, ψ) and gyro biases ($b_{\omega_x}, b_{\omega_y}, b_{\omega_z}$). Gyroscope readings, $\omega_g = (\omega_{g,x}, \omega_{g,y}, \omega_{g,z})$, are utilized as inputs in the process model, and accelerometer and magnetometer readings are considered as measurements. By considering the gyro biases as constant or slowly varying signals, process and measurement models can be written as

$$\begin{bmatrix} \dot{\phi} \\ \dot{\theta} \\ \dot{\psi} \\ \dot{b}_{\omega_x} \\ \dot{b}_{\omega_y} \\ \dot{b}_{\omega_z} \end{bmatrix} = \begin{bmatrix} \begin{bmatrix} 1 & s_\phi t_\theta & c_\phi t_\theta \\ 0 & c_\phi & -s_\phi \\ 0 & s_\phi \sec\theta & c_\phi \sec\theta \end{bmatrix} \begin{bmatrix} \omega_{g,x} - b_{\omega_x} \\ \omega_{g,y} - b_{\omega_y} \\ \omega_{g,z} - b_{\omega_z} \end{bmatrix} \\ 0 \\ 0 \\ 0 \end{bmatrix} + w(t) \quad (16)$$

$$z = \begin{bmatrix} f_{acc,x} \\ f_{acc,y} \\ f_{acc,z} \\ \psi_{mag} \end{bmatrix} = \begin{bmatrix} \omega_{g,x} - b_{\omega_x} \\ \omega_{g,y} - b_{\omega_y} \\ \omega_{g,z} - b_{\omega_z} \\ \psi \end{bmatrix} \times V_{ref} - g \begin{bmatrix} -s_\theta \\ s_\phi c_\theta \\ c_\phi c_\theta \end{bmatrix} + v(t) \quad (17)$$

where $\omega_{g,x}, \omega_{g,y}$ and $\omega_{g,z}$ are angular velocity measurements of 3-axis gyroscope around x, y and z axes, $f_{acc} = (f_{acc,x}, f_{acc,y}, f_{acc,z})$ are specific forces measured by 3-axis accelerometer along x, y, and z axes, and ψ_{mag} is the yaw angle obtained from the raw measurements of the 3-axis magnetometer. V_{ref} is the linear velocity vector expressed in body frame and can be measured either by GPS, or vision based motion capture system, or pitot tube. We should note that $V_{ref} = 0$ for a hovering quadrotor. Finally, $w(t)$ and $v(t)$ are the process and measurement noises, respectively, and they are assumed to be additive white Gaussian noises with known covariances.

Once attitude angles and gyro biases are estimated by the extended Kalman filter (EKF) which utilizes process and measurement models given in (16) and (17), the estimated gyro biases are subtracted from the gyro measurements, and the resulting compensated angular velocity is used as a measurement in a classical Kalman filter (KF) as shown Fig. 2.

To estimate the angular velocity $\omega = [p, q, r]^T$ and angular acceleration $\alpha = [\dot{p}, \dot{q}, \dot{r}]^T$ in the body frame, instead of using numerical differentiation which amplifies noise, a classical Kalman filter (KF) is employed to avoid amplification of noise and provide much smoother results. Process and measurement models for the underlying Kalman filter are given by (18) and (19):

$$\begin{bmatrix} \dot{\omega} \\ \dot{\alpha} \end{bmatrix} = \begin{bmatrix} I_{3 \times 3} & TI_{3 \times 3} \\ 0_{3 \times 3} & I_{3 \times 3} \end{bmatrix} \begin{bmatrix} \omega \\ \alpha \end{bmatrix} + \begin{bmatrix} 0.5T^2 I_{3 \times 3} \\ TI_{3 \times 3} \end{bmatrix} \underbrace{\gamma}_{\triangleq w_k} \quad (18)$$

where angular jerk, $\gamma = [\ddot{p}, \ddot{q}, \ddot{r}]^T$ is treated as a stochastic input (w_k), which is assumed to be additive white Gaussian noise, applied to the system.

Compensated gyroscope readings, $\omega_g - \hat{b}_\omega$, are used as measurements in the following measurement model:

$$z = \omega_g - \hat{b}_\omega = \begin{bmatrix} I_{3 \times 3} & 0_{3 \times 3} \end{bmatrix} \begin{bmatrix} \omega \\ \alpha \end{bmatrix} + v_k \quad (19)$$

where v_k is the colored measurement noise due to the cascaded structure of the overall filter and utilization of estimated gyro biases in (19). Since the measurement noise is no longer white, KF lacks its optimality. One can use Inverse ϕ -Algorithm [27] to deal with colored measurement noise. However, in this work, a KF is employed for estimation.

Since the attitude dynamics of the quadrotor is controlled with respect to inertial frame, estimated angular velocity and accelerations must be transformed into Euler rates and accelerations, which is the final step in the proposed cascaded method (Fig. 2). The bottom-right 3×3 submatrix of the Jacobian in (4), denoted by $\mathbb{B}(\phi, \theta)$, transforms angular

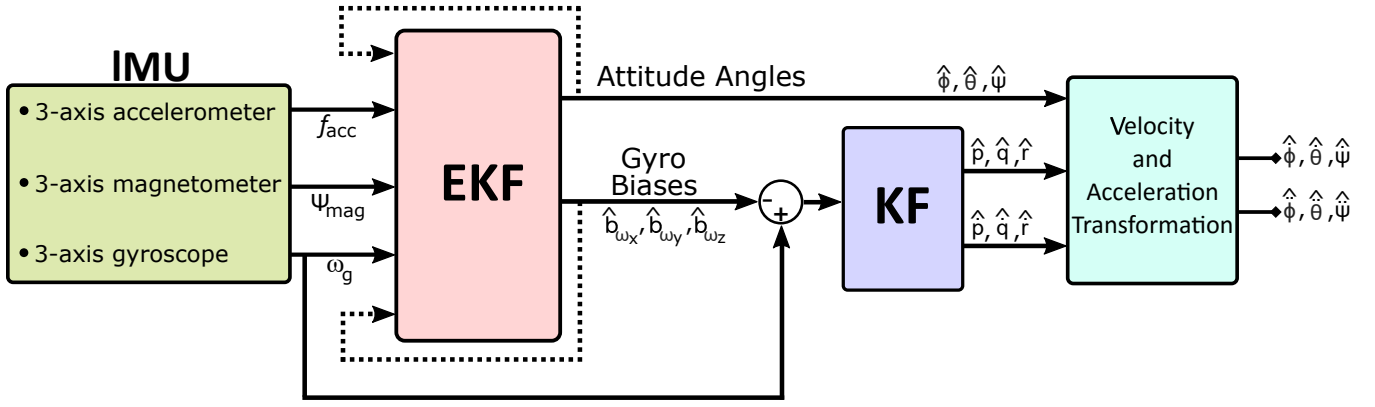


Fig. 2. Estimation of Euler angles, rates and accelerations

velocities into Euler angular rates as

$$\hat{\Omega} = \begin{bmatrix} \hat{\phi} \\ \hat{\theta} \\ \hat{\psi} \end{bmatrix} = \mathbb{B}(\hat{\phi}, \hat{\theta}) \begin{bmatrix} \hat{p} \\ \hat{q} \\ \hat{r} \end{bmatrix} \quad (20)$$

In order to transform angular accelerations, $\mathbb{B}(\phi, \theta, \dot{\phi}, \dot{\theta})$ is also needed and can be written explicitly as

$$\mathbb{B} = \begin{bmatrix} 0 & \dot{\phi} c_{\phi} t_{\theta} + s_{\phi} \dot{\theta} \sec^2_{\theta} & -\dot{\phi} s_{\phi} t_{\theta} + c_{\phi} \dot{\theta} \sec^2_{\theta} \\ 0 & -\dot{\phi} s_{\phi} & -\dot{\phi} c_{\phi} \\ 0 & \frac{\dot{\phi} c_{\phi} c_{\theta} + s_{\phi} \dot{\theta} s_{\theta}}{c_{\theta}^2} & \frac{-\dot{\phi} s_{\phi} c_{\theta} + c_{\phi} \dot{\theta} s_{\theta}}{c_{\theta}^2} \end{bmatrix} \quad (21)$$

Finally, Euler angular accelerations in the inertial frame can be estimated as

$$\hat{\Gamma} = \begin{bmatrix} \hat{\phi} \\ \hat{\theta} \\ \hat{\psi} \end{bmatrix} = \mathbb{B}(\hat{\phi}, \hat{\theta}, \hat{\phi}, \hat{\theta}) \begin{bmatrix} \hat{p} \\ \hat{q} \\ \hat{r} \end{bmatrix} + \mathbb{B}(\hat{\phi}, \hat{\theta}) \begin{bmatrix} \hat{p} \\ \hat{q} \\ \hat{r} \end{bmatrix} \quad (22)$$

IV. HOVERING CONTROL OF THE QUADROTOR USING ACCELERATION FEEDBACK

When a quadrotor is in hovering mode, it is desired that the vehicle should stay at a reference position (X^d, Y^d, Z^d) or in its immediate vicinity, and its angular rates must be very close to zero. This is achieved by designing separate position and attitude controllers.

A. Position Controller

In order to reject disturbances acting on the positional dynamics of the quadrotor, we designed an acceleration based disturbance observer (ABDOB) (Fig. 3) that estimates the total disturbance that includes external disturbances, nonlinear terms and parametric uncertainties. Note that the mass-inertia matrix of the quadrotor can be written as $M = M_{nom} + \tilde{M}$ where M_{nom} is the diagonal nominal mass-inertia matrix and \tilde{M} is the difference between actual and nominal inertia matrices. By using nominal inertia matrix explicitly, (1) can be rewritten as

$$M_{nom} \dot{\zeta} = f + \tau_{dist} \quad (23)$$

where f and τ_{dist} are the system actuator vector and the total disturbance, respectively, and they are defined as

$$f = E(\xi) \omega^2 \quad (24)$$

$$\tau_{dist} = -\tilde{M} \dot{\zeta} - C(\zeta) \zeta + G + O(\zeta) \Omega + D(\zeta, \xi) \quad (25)$$

Estimating the total disturbance from (25) is not an easy task due to many unknowns and uncertainties. However, it could be estimated from (23) if the acceleration signal $\dot{\zeta}$ were available. So, using an estimate of the acceleration, $\hat{\zeta}$, the total disturbance, τ_{dist} , can be estimated as

$$\hat{\tau}_{dist_i} = M_{nom} \hat{\zeta} - f \quad (26)$$

where $i = 1, \dots, 6$. Usually a low-pass filter $G(s) = \frac{s}{s^2 + s}$ is employed in the implementation and the right-hand side of (26) is filtered by $G(s)$. Finally, estimated total disturbance is subtracted from the virtual control inputs that control positional dynamics of the quadrotor as detailed below.

To design the virtual control inputs, errors along X , Y and Z axes and their derivatives can be written as

$$e_X = X^d - X(t) \Rightarrow \dot{e}_X = -\dot{X}(t) \quad (27)$$

$$e_Y = Y^d - Y(t) \Rightarrow \dot{e}_Y = -\dot{Y}(t) \quad (28)$$

$$e_Z = Z^d - Z(t) \Rightarrow \dot{e}_Z = -\dot{Z}(t) \quad (29)$$

Positional control of the vehicle boils down to the control of double integrators through the following virtual controls:

$$\mu_X = K_{p,X} e_X + K_{d,X} \dot{e}_X + K_{i,X} \int_0^t e_X dt - \hat{\tau}_{dist_1} \quad (30)$$

$$\mu_Y = K_{p,Y} e_Y + K_{d,Y} \dot{e}_Y + K_{i,Y} \int_0^t e_Y dt - \hat{\tau}_{dist_2} \quad (31)$$

$$\mu_Z = K_{p,Z} e_Z + K_{d,Z} \dot{e}_Z + K_{i,Z} \int_0^t e_Z dt - \hat{\tau}_{dist_3} \quad (32)$$

where desired feedforward accelerations are 0 due to constant X^d, Y^d and Z^d . Using simple trigonometric relations, these virtual controls can be transformed into the total thrust u_1 , and the desired roll ϕ^d , and pitch θ^d angles as

$$u_1 = m \sqrt{\mu_X^2 + \mu_Y^2 + (\mu_Z + g)^2} \quad (33)$$

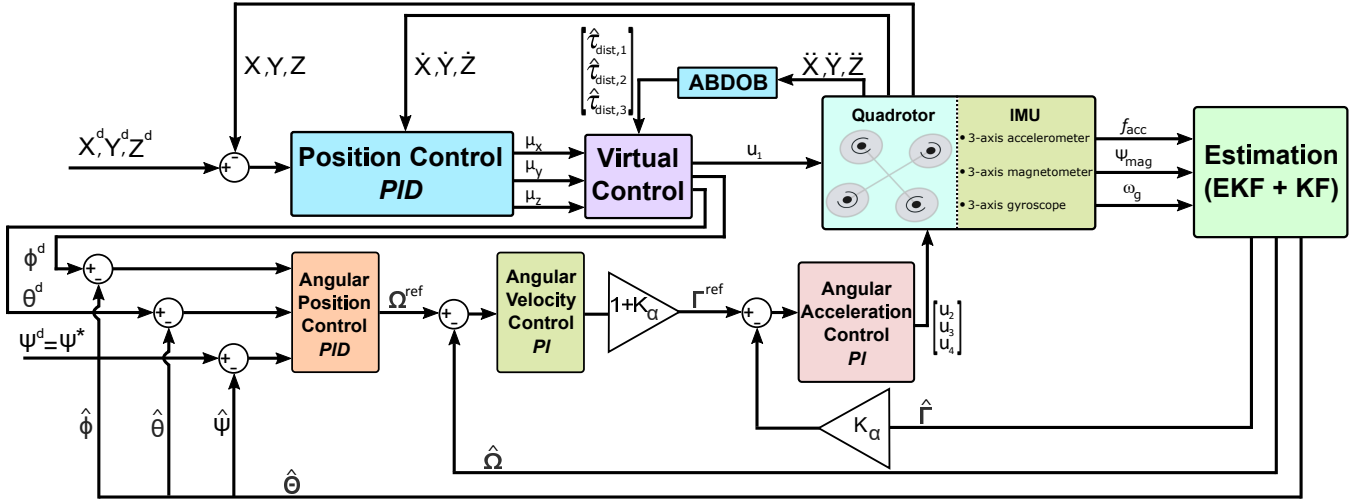


Fig. 3. Overall hovering control architecture

$$\phi^d = \text{asin}\left(\frac{-\mu_y}{\sqrt{\mu_x^2 + \mu_y^2 + (\mu_z + g)^2}}\right) \quad (34)$$

$$\theta^d = \text{asin}\left(\frac{\mu_x}{\cos(\phi^d) + \sqrt{\mu_x^2 + \mu_y^2 + (\mu_z + g)^2}}\right) \quad (35)$$

Remark 1: To obtain an estimate of the linear accelerations along X, Y and Z axes in the world frame, body linear accelerations measured by a 3-axis accelerometer are transformed by the orientation of the quadrotor with respect to the world frame and the acceleration due to the gravity is subtracted. The orientation of the quadrotor with respect to the world frame is estimated using the EKF outlined in Section III. The resulting linear acceleration in the world frame is integrated to obtain an estimate of the linear velocity, and integration of the linear velocity gives the estimate of the linear position. It should be noted that drift problems occur in practical applications due to the integration of offsets and/or noises in measured signals and therefore these estimates must be corrected by some external sensors such as GPS or camera.

Remark 2: It should be noted the acceleration based disturbance observer (ABDOB) estimates 6 disturbance components, and therefore disturbance moments can also be estimated in addition to disturbance forces. However, in this work we consider first three components of $\hat{\tau}_{dist}$ for disturbance rejection in the positional dynamics. In the attitude control, we will design angular acceleration based controllers that utilize estimated angular accelerations from Section III.

B. Attitude Controller

In order to achieve robust hovering performance, disturbance torques/moments acting on the attitude dynamics of the vehicle must be rejected as much as possible. To

capture and compensate for the effects of the disturbances, acceleration feedback is introduced into the inner loop of the attitude controller (Fig. 3).

By taking ϕ^d and θ^d angles determined from (34) and (35) into account and by setting $\psi^d = \psi^*$ (some constant heading), errors in attitude angles can be defined as

$$e_\phi = \phi^d - \hat{\phi}(t) \quad (36)$$

$$e_\theta = \theta^d - \hat{\theta}(t) \quad (37)$$

$$e_\psi = \psi^d - \hat{\psi}(t) \quad (38)$$

Angular position controllers are designed as PID controllers and output of these controllers provide references $\Omega^{ref} = [\phi^{ref}, \theta^{ref}, \psi^{ref}]^T$ for angular velocity control loops as

$$\dot{\phi}^{ref} = K_{p,\phi} e_\phi + K_{d,\phi} \dot{e}_\phi + K_{i,\phi} \int_0^t e_\phi dt \quad (39)$$

$$\dot{\theta}^{ref} = K_{p,\theta} e_\theta + K_{d,\theta} \dot{e}_\theta + K_{i,\theta} \int_0^t e_\theta dt \quad (40)$$

$$\dot{\psi}^{ref} = K_{p,\psi} e_\psi + K_{d,\psi} \dot{e}_\psi + K_{i,\psi} \int_0^t e_\psi dt \quad (41)$$

By employing estimated angular velocities as feedback signals, angular velocity errors and the resulting PI controllers are developed as

$$e_\Omega = \Omega^{ref} - \hat{\Omega} \quad (42)$$

$$\Gamma^{ref} = (1 + K_\alpha)(K_{p,\Omega} e_\Omega + K_{i,\Omega} \int_0^t e_\Omega dt) \quad (43)$$

Feedback errors for acceleration control are then defined as

$$e_\Gamma = \Gamma^{ref} - K_\alpha \Gamma \quad (44)$$

where K_α is the acceleration gain, which can be thought of as electronic inertia. It increases the effective inertia by a factor of $1 + K_\alpha$. Increasing the effective inertia leads to high dynamic stiffness and better disturbance rejection. As emphasized in [28], the increase in effective inertia actually

reduces loop gain, hence reducing system response rates. The benefits of acceleration feedback are realized when control-loop gains are scaled up by the amount that the inertia increases, that is, by the factor $1 + K_\alpha$. This is why PI controller gains are scaled by $1 + K_\alpha$ in (43).

Finally, input torques are designed as PI controllers, namely

$$u_{2,3,4} = K_{p,\Gamma} e_\Gamma + K_{i,\Gamma} \int_0^t e_\Gamma dt \quad (45)$$

V. SIMULATION RESULTS AND DISCUSSIONS

In this section, simulation results of the proposed acceleration feedback control (AFC) technique will be presented and compared with the controller that does not employ such feedback. Simulations are performed on a high fidelity simulation model where sensor imperfections, e.g. sensor biases and noises, are also taken into account. More precisely, measurements are corrupted by constant biases and additive white Gaussian noises.

Model parameters used in simulations are tabulated in Table I (see [25] for details).

TABLE I
MODELING PARAMETERS

Symbol	Description	Magnitude
m	mass	4.5 kg
l_s	Rotor distance to cog along y axis	0.3 m
l_l	Rotor distance to cog along x axis	0.3 m
I_{xx}	Moment of inertia along x axis	0.405 kg m ²
I_{yy}	Moment of inertia along y axis	0.405 kg m ²
I_{zz}	Moment of inertia along z axis	0.72 kg m ²
λ	Torque/force ratio	0.01 Nm/N

Position and attitude tracking performances are depicted in Fig. 4 and Fig. 5. RMS values of errors and maximum errors belong to hovering and attitude performances are tabulated in Table II. These results show that the performance is dramatically improved in both positioning and attitude tracking, and the quadrotor can hover at or in the vicinity of a given point despite the disturbance forces and moments generated by the Dryden wind model (Fig. 6 and Fig. 7). In generating aerodynamic forces and moments, the multiplicative factors which scale wind velocities in this model are chosen as 1.2 and 0.9 for linear and rotational velocities, respectively.

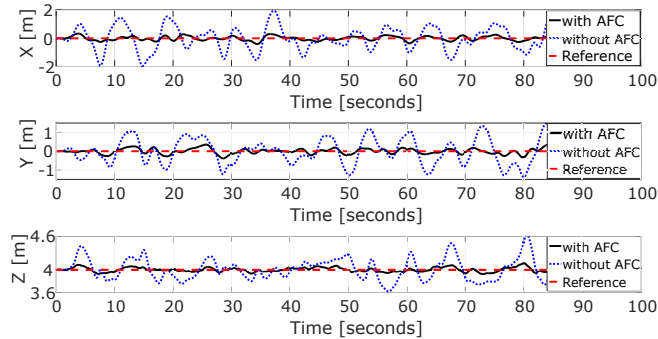


Fig. 4. Position tracking performance with and without acceleration feedback

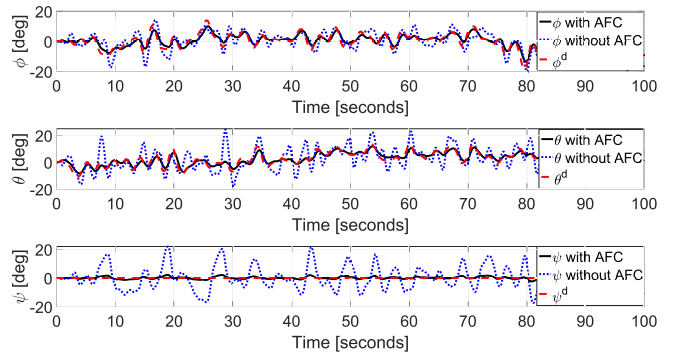


Fig. 5. Attitude tracking performance with and without acceleration feedback

TABLE II
HOVERING AND ATTITUDE TRACKING PERFORMANCES

Criteria	without AFC	with AFC
$RMS(e_X)$	0.805 m	0.152 m
$max(e_X)$	1.963 m	0.403 m
$RMS(e_Y)$	0.674 m	0.140 m
$max(e_Y)$	1.663 m	0.385 m
$RMS(e_Z)$	0.196 m	0.039 m
$max(e_Z)$	0.618 m	0.121 m
$RMS(e_\phi)$	4.214°	2.055°
$max(e_\phi)$	12.175°	6.999°
$RMS(e_\theta)$	6.335°	1.943°
$max(e_\theta)$	25.191°	5.109°
$RMS(e_\psi)$	8.108°	0.846°
$max(e_\psi)$	21.935°	2.371°

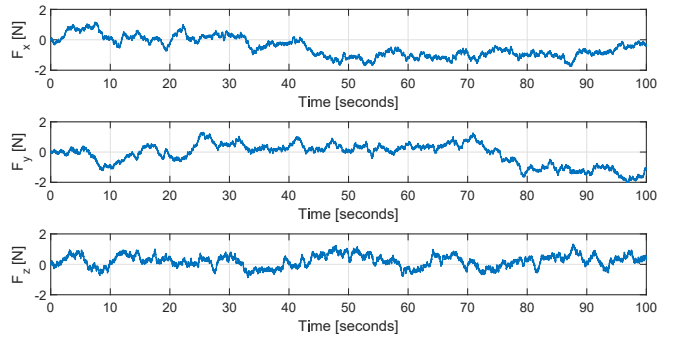


Fig. 6. Wind forces acting on the quadrotor generated by Dryden model

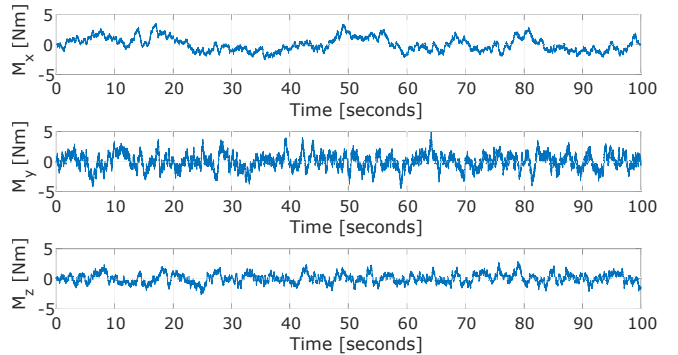


Fig. 7. Wind moments acting on the quadrotor generated by Dryden model

Estimated disturbances by ABDOB are shown in Fig. 8. Fig. 6 and Fig. 8 shows that estimated disturbances are very similar to the wind forces acting on the system. Successful estimation of the disturbance forces provides improved hovering performance as shown in Fig. 4. Thrust forces generated by motors with acceleration feedback are depicted in Fig. 9 and show that the input forces are within the physical limits.

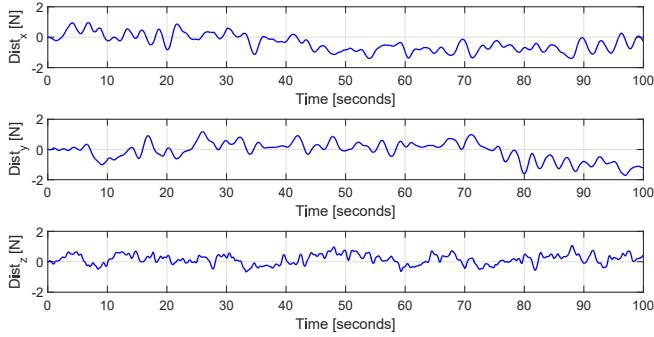


Fig. 8. Estimated disturbances acting on the positional dynamics of the quadrotor by ABDOB

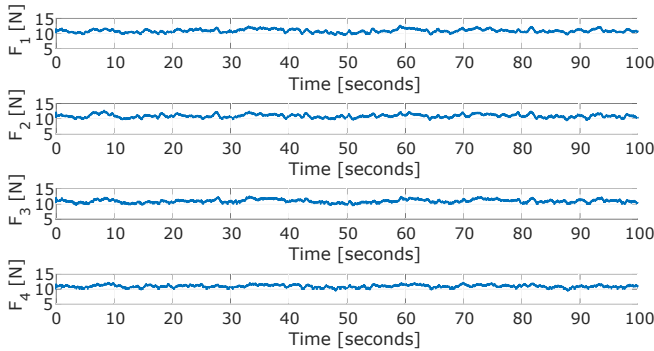
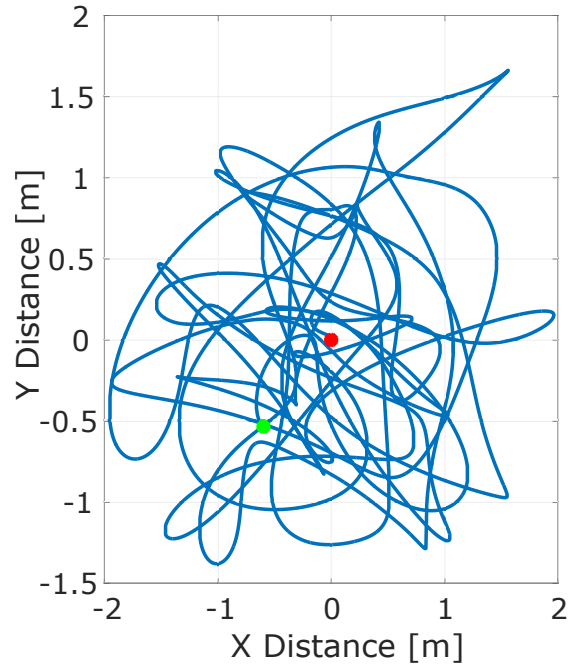


Fig. 9. Motor thrust forces with acceleration feedback

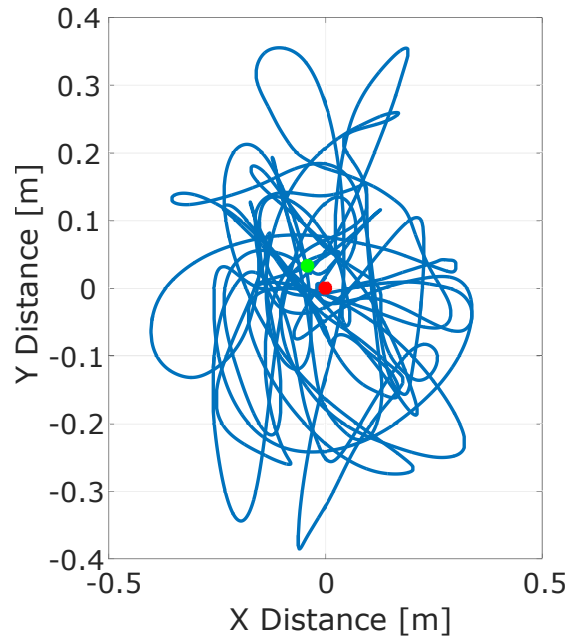
Finally, Fig. 10 presents the motion of the quadrotor in the horizontal x - y plane and shows that hovering without acceleration feedback can be achieved in a 14 m^2 area whereas proposed method can provide more robust hovering in an area of less than 0.8 m^2 under the same windy conditions. Red and green points in Fig. 10 are the initial and final positions of the quadrotor in the x - y plane, respectively.

VI. CONCLUSION AND FUTURE WORK

We have now presented a robust hovering control method for a quadrotor which utilizes acceleration feedback to reject disturbances acting on both positional and attitude dynamics. In order to achieve high dynamic stiffness against disturbance forces and moments, an acceleration based disturbance observer (ABDOB) is employed in the positional control and a nested angular position, velocity and acceleration control structure is utilized in the attitude control of the quadrotor. Reliable angular accelerations are obtained by fusing the raw measurements from an IMU, that includes a 3-axis gyroscope, a 3-axis accelerometer and a 3-axis magnetometer, in



(a)



(b)

Fig. 10. Hovering performance without (a) and with (b) acceleration feedback (motion in the horizontal x - y plane)

a cascaded estimation framework that utilizes an extended Kalman filter and a classical Kalman filter. Estimated Euler accelerations are employed in the attitude control loops. By using a high fidelity simulation model which also takes uncertainties, e.g. biases and noises, in sensor measurements into account, it is shown that the performance of hovering controller that employs estimated accelerations as feedback signals is improved dramatically. This is basically due to

the increasing effective inertia of the system which implies higher dynamic stiffness against external disturbances.

As future work, proposed method will be extended to the trajectory control of the quadrotor and its performance will also be tested in real-flight experiments.

REFERENCES

- [1] C. Hancer, K.T. Oner, E. Sirimoglu, E. Cetinsoy and M. Unel, "Robust hovering control of a quad tilt-wing uav", *In IECON 2010-36th Annual Conference on IEEE Industrial Electronics Society*, pp. 1615-1620, 2010.
- [2] C. Hancer, K. T. Oner, E. Sirimoglu, E. Cetinsoy and M. Unel, "Robust position control of a tilt-wing quadrotor", *In Decision and Control (CDC), 2010 49th IEEE Conference on*, pp. 4908-4913, 2010.
- [3] R. Zhang, Q. Quan and K. Y. Cai, "Attitude control of a quadrotor aircraft subject to a class of time-varying disturbances", *Control Theory and Applications, IET*, 5(9), 1140-1146, 2011.
- [4] S.L. Waslander and C. Wang, "Wind disturbance estimation and rejection for quadrotor position control", *In AIAA Infotech@ Aerospace Conference and AIAA Unmanned... Unlimited Conference*, 2009.
- [5] A. Tayebi and S. McGilvray, "Attitude stabilization of a VTOL quadrotor aircraft", *IEEE Transactions on control systems technology*, 14(3), 562-571, 2006.
- [6] J. Kim, M. S. Kang and S. Park, "Accurate modeling and robust hovering control for a quad-rotor VTOL aircraft", *In Selected papers from the 2nd International Symposium on UAVs*, pp. 9-26, 2009.
- [7] Y. Yildiz, M. Unel and A. E. Demirel, "Adaptive nonlinear hierarchical control of a quad tilt-wing UAV", *In Control Conference (ECC)*, pp. 3623-3628, 2015.
- [8] Y. Yildiz, M. Unel, A. E. Demirel, "Nonlinear Hierarchical Control of a Quad-Tilt-Wing UAV: An Adaptive Control Approach", *International Journal of Adaptive Control and Signal Processing*, DOI:10.1002/acs2759, 2017.
- [9] D. Cabecinhas, C. Rita, S. Carlos Silvestre, "A globally stabilizing path following controller for rotorcraft with wind disturbance rejection", *IEEE Transactions on Control Systems Technology* 23 (2) 708-714, 2015.
- [10] K. Rudin, M. D. Hua, G. Ducard and S. Bouabdallah, "A robust attitude controller and its application to quadrotor helicopters", *In 18th IFAC World Congress*, 10379-10384, 2011.
- [11] P. Pounds, T. Hamel and R. Mahony, "Attitude control of rigid body dynamics from biased IMU measurements", *In Decision and Control, 46th IEEE Conference on*, pp. 4620-4625, 2007.
- [12] L. G. Carrillo, A. Dzul and R. Lozano, "Hovering quad-rotor control: A comparison of nonlinear controllers using visual feedback", *Aerospace and Electronic Systems, IEEE Transactions on*, 48(4), 3159-3170, 2012.
- [13] K. Mathe and L. Busoniu, "Vision and control for UAVs: A survey of general methods and of inexpensive platforms for infrastructure inspection", *Sensors*, 15(7), 14887-14916, 2015.
- [14] X. Bin, L. Yang, Z. Xu, C. A. O. Meihui and W. Fu, "Hovering control of a nano quadrotor unmanned aerial vehicle using optical flow", *In Control Conference (CCC), 33rd Chinese*, pp. 8259-8264, 2014.
- [15] H. Lim, H. Lee, H and J. Kim, "Onboard flight control of a micro quadrotor using single strapdown optical flow sensor", *In Intelligent Robots and Systems (IROS), IEEE/RSJ International Conference on*, pp. 495-500, 2012.
- [16] S. Azrad, F. Kendoul, D. Perbrianti and K. Nonami, "Visual servoing of an autonomous micro air vehicle for ground object tracking", *In Intelligent Robots and Systems (IROS) IEEE/RSJ International Conference on*, pp. 5321-5326, 2009.
- [17] Y. Hori, "Disturbance suppression on an acceleration control type DC servo system", *In Power Electronics Specialists Conference, 19th Annual IEEE*, pp. 222-229, 1988.
- [18] Y. Hori, "Position and mechanical impedance control method of robot actuators based on the acceleration control", *In Power Electronics Specialists Conference, 20th Annual IEEE*, pp. 423-430, 1989.
- [19] P. B. Schmidt and R. D. Lorenz, "Design principles and implementation of acceleration feedback to improve performance of DC drives", *Industry Applications, IEEE Transactions on*, 28(3), 594-599, 1992.
- [20] J. D. Han, Y. Q. He and W. L. Xu, "Angular acceleration estimation and feedback control: An experimental investigation", *Mechatronics*, 17(9), 524-532, 2007.
- [21] T. Insperger, J. Milton and G. Stepan, "Acceleration feedback improves balancing against reflex delay", *Journal of the Royal Society Interface*, 10(79), 2013.
- [22] T. Tomic, "Evaluation of acceleration-based disturbance observation for multicopter control", *European Control Conference*, 2014.
- [23] S. H. Jeong, S. Jung and M. Tomizuka, "Attitude control of a quadrotor system using an acceleration-based disturbance observer: An empirical approach", *In Advanced Intelligent Mechatronics (AIM), IEEE/ASME International Conference on*, pp. 916-921, 2012.
- [24] K. T. Oner, E. Cetinsoy, E. Sirmoglu, C. Hancer, M. Unel, M. F. Aksit, "Mathematical Modeling and Vertical Flight Control of a Tilt-Wing UAV", *Turkish Journal of Electrical Engineering and Computer Sciences*, 20 (1), 149-157, 2012
- [25] E. Cetinsoy, S. Dikyar, C. Hancer, K. T. Oner, E. Sirimoglu, M. Unel, M. F. Aksit, "Design and construction of a novel quad tilt-wing UAV", *Mechatronics*, 22(6), 723-745, 2012.
- [26] P. S. Maybeck, "Stochastic models, estimation", 1982.
- [27] M. G. Petovello, K. OKeefe, G. Lachapelle, M. E. Cannon, "Consideration of time-correlated errors in a Kalman filter applicable to GNSS", *Journal of Geodesy*, 83(1), 51-56 2009.
- [28] F. Tian, K. Craig and M. Nagurka, "Disturbance attenuation in a magnetic levitation system with acceleration feedback", *IEEE International Conference on Industrial Technology (ICIT)*, pp. 59-64, 2011.